

Cycle-to-Cycle Intrinsic RESET Statistics in HfO₂-Based Unipolar RRAM Devices

Shibing Long, *Member, IEEE*, Xiaojuan Lian, Tianchun Ye, Carlo Cagli, Luca Perniola, Enrique Miranda, *Senior Member, IEEE*, Ming Liu, *Senior Member, IEEE*, and Jordi Suñé, *Fellow, IEEE*

Abstract—The statistics of the RESET voltage (V_{RESET}) and the RESET current (I_{RESET}) of Pt/HfO₂/Pt resistive random access memory (RRAM) devices operated under unipolar mode are analyzed. The experimental results show that both the distributions of I_{RESET} and V_{RESET} are strongly influenced by the distribution of initial resistance in the ON state (R_{ON}), which is related to the size of the conductive filament (CF) before RESET. By screening the statistical data into different resistance ranges, both the distributions of I_{RESET} and V_{RESET} are shown to be compatible with a Weibull model. Contrary to previous reports for NiO-based RRAM, the Weibull slopes of the I_{RESET} and V_{RESET} are demonstrated to be independent of R_{ON} . This is an indication that the RESET point, defined in this letter as the point of maximum current, corresponds to the initial phase of CF dissolution. On the other hand, given that the scale factor of the V_{RESET} distribution ($V_{RESET63\%}$) is roughly independent of R_{ON} , the scale factor of the I_{RESET} ($I_{RESET63\%}$) is inversely proportional to R_{ON} . This is analogous to what was found in NiO-based RRAM and it is consistent with the thermal dissolution model of RESET. Our results highlight the intrinsic link between the SET and RESET statistics and the need for controlling the variation of ON-state resistance to reduce the variability of the RESET voltage and current.

Index Terms—RESET statistics, resistive random access memory (RRAM), resistive switching (RS).

I. INTRODUCTION

AS A PROMISING candidate for next-generation non-volatile and storage-class memories, the resistive random access memory (RRAM), which is based on the resistive switching (RS) phenomenon in transition metal oxides, has been intensively investigated recently. The reasons for this interest are the simple structure of the devices, their good scalability, high speed, and good compatibility with silicon CMOS

Manuscript received September 9, 2012; accepted February 28, 2013. Date of publication April 3, 2013; date of current version April 22, 2013. This work was supported in part by Spanish Ministry of Science and Technology under Contract TEC2012-32305 (Partially funded by the European Union FEDER Program), the DURSI of the Generalitat de Catalunya under Contract 2009SGR783, the Ministry of Science and Technology of China under Grant 2010CB934200, Grant 2011CBA00602, Grant 2009CB930803, Grant 2011CB921804, Grant 2011AA010401, and Grant 2011AA010402 and the National Natural Science Foundation of China under Grant 61221004, Grant 61274091, Grant 60825403, Grant 61106119, and Grant 61106082. The review of this letter was arranged by Editor T. Wang.

S. Long, T. Ye, and M. Liu are with the Lab of Nanofabrication and Novel Devices Integration, Institute of Microelectronics, Chinese Academy of Sciences, Beijing 100029, China (e-mail: tcye@ime.ac.cn; liuming@ime.ac.cn).

X. Lian, E. Miranda, and J. Suñé are with the Departament d'Enginyeria Electrònica, Universitat Autònoma de Barcelona, Bellaterra 08193, Spain.

C. Cagli and L. Perniola are with CEA, LETI, Grenoble F-38054, France.

Color versions of one or more of the figures in this letter are available online at <http://ieeexplore.ieee.org>.

Digital Object Identifier 10.1109/LED.2013.2251314

technology [1]–[4]. HfO₂ has been used in the gate dielectric stack of CMOS devices starting from the 32-nm technology node. Hence, it might be one of the most competitive RS functional materials for RRAM [5]–[8]. However, the wide cycle-to-cycle and cell-to-cell fluctuation of RS parameters such as the SET/RESET voltage and current, and the ON/OFF resistances still represent a significant barrier to engineer RRAM into large-scale commercial manufacturing [9]–[11]. In this letter, we present the characterization of the statistics of RESET voltage and current correlated to the statistics of ON-state resistance in HfO₂-based RRAM. The operation of these devices involves the creation and dissolution of a conductive filament (CF), likely related to oxygen vacancies.

II. EXPERIMENTAL SETUP

Pt/HfO₂/Pt structures were fabricated with a 10-nm-thick HfO₂ RS layer deposited by atomic layer deposition at 350 °C. The Pt bottom (BE) and top (TE) electrodes were prepared by physical vapor deposition. TE was patterned by etching a square area of 1 μm². The RESET statistics were studied by cycling five individual devices for 1250 successive SET/RESET cycles each. Currents and voltages were measured by an Agilent 4155C semiconductor parameter analyzer which was also used to apply positive voltage ramp stress to the TE with the BE connected to ground. During the SET transition, a 1-mA current compliance limit was used to avoid the occurrence of hard dielectric breakdown, which would otherwise destroy the device.

III. RESULTS AND DISCUSSION

The fabricated Pt/HfO₂/Pt devices were operated in the unipolar mode. As shown in Fig. 1(a), the RESET point (V_{RESET} , I_{RESET}) is defined as the maximum of the RESET current [10], [11]. The raw voltage and current data were corrected by the series resistance R_S , which was estimated to be ~28 Ω by adding the resistance of the experimental setup (~18 Ω) to the Maxwell resistance, estimated to be ~10 Ω for a CF with a diameter of ~10 nm. After this correction, the RESET voltage V_{RESET} appears to be rather independent of R_{ON} [Fig. 1(b)], and the RESET current I_{RESET} [inset of Fig. 1(b)] is inversely proportional to R_{ON} . This behavior is completely analogous to what was previously reported for NiO-based RRAM devices [10], [11] and it is compatible with the predictions of the thermal dissolution model of RESET [12], [13]. In this model, RESET is considered to occur by the out-diffusion of the conducting defects (i.e., oxygen vacancies) when the local CF temperature

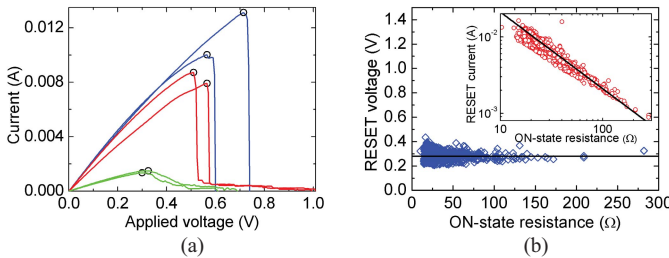


Fig. 1. (a) Six typical I - V curves during dc RESET voltage sweeping of a Pt/HfO₂/Pt device showing progressive RESET (green and red curves) and abrupt RESET (blue curves) events. The black circles represent the RESET points. (b) V_{RESET} - R_{ON} and I_{RESET} - R_{ON} (inset) scatter plots of the measured 1250 cycles of the same device after data correction by the series resistance $R_S = 28 \Omega$.

reaches a critical value T_{RESET} . Taking into account the balance between Joule dissipation and heat evacuation, the basic equation of the model is $T_{\text{RESET}} = T_0 + (R_{\text{TH}}/R_{\text{ON}})V_{\text{RESET}}^2$, where T_0 is the operation temperature and R_{TH} is the thermal resistance describing heat dissipation from the CF to the environment [12], [13]. If R_{ON} is low enough, $R_{\text{TH}} \propto R_{\text{ON}}$ due to the Wiedemann–Franz law, and V_{RESET} is predicted to be independent of R_{ON} , as found in our experiments [Fig. 1(b)]. V_{RESET} being independent of R_{ON} , it follows that I_{RESET} is proportional to $1/R_{\text{ON}}$, as found in the inset of Fig. 1(b).

Due to the statistical variation of R_{ON} , we use a data screening method to get the V_{RESET} and I_{RESET} distributions in different R_{ON} ranges. Fig. 2 shows the global cumulative distribution of V_{RESET} and I_{RESET} together with the screened distributions for the different R_{ON} ranges. In both cases, the distributions have been displayed in the Weibull plot. Since the screened cumulative distributions are straight lines in these plots, we conclude that they are compatible with Weibull distributions. The Weibull distribution $F = 1 - \exp[-(x/x_{63\%})^\beta]$ is described by two parameters, the scale factor $x_{63\%}$, which is the value of the statistical variable at $F \approx 0.63$, and the shape factor or Weibull slope β , which measures the statistical dispersion (similar to the standard deviation in the normal distribution). If we compare the global distributions of V_{RESET} and I_{RESET} with the screened distributions, we find that the shape of the global distribution has nothing to do with the intrinsic dispersion of the RESET results. We have verified that if the screened distributions are combined with adequate statistical weights according to the number of samples in each resistance range, the original global cumulative distributions of V_{RESET} and I_{RESET} are nicely reproduced. This confirms the consistency of our screening method. In particular, the change of slope in the global I_{RESET} distribution is perfectly reproduced, thus emphasizing that the shape of this global distribution is fully controlled by the distribution of R_{ON} . In fact, the change of slope is only related to the fact that the probability of finding R_{ON} within the two lowest resistance ranges (i.e., between 15 and 25 Ω) is much higher than for higher R_{ON} values, because I_{RESET} decreases monotonically with R_{ON} and has a narrow spread in each R_{ON} value as shown in the inset of Fig. 1(b). According to these results, we can conclude that the shape of the global distributions of V_{RESET} and I_{RESET} does not provide useful insight about the intrinsic statistics of the RESET process unless we get rid of the variations of R_{ON} . On the other hand, Fig. 2 demonstrates that a steep distribution of I_{RESET} can be obtained by

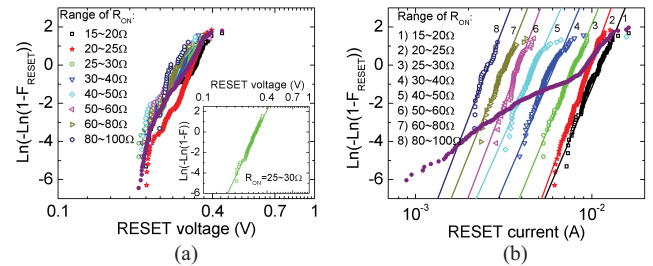


Fig. 2. Experimental distributions (symbols) of the same device and fitting of (a) V_{RESET} and (b) I_{RESET} to Weibull distributions (lines) as a function of R_{ON} . The extreme R_{ON} ranges ($R_{\text{ON}} < 15 \Omega$ and $R_{\text{ON}} > 100 \Omega$) are not included in these plots because of the limited number of points which yield distorted distributions. The purple dots show the global distribution of V_{RESET} and I_{RESET} of all the 1250 cycles.

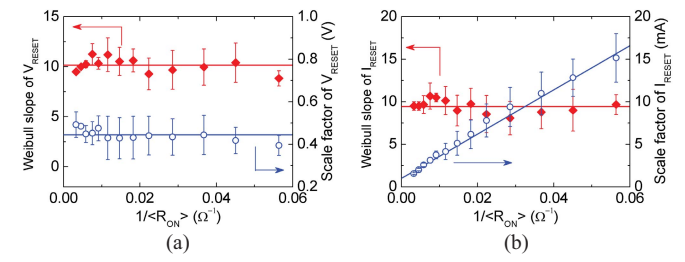


Fig. 3. R_{ON} dependence of the shape and scale factors of the (a) V_{RESET} and (b) I_{RESET} distributions of five different devices. The straight lines show the fitting results. $\langle R_{\text{ON}} \rangle$ is the average of R_{ON} in each screening range. Each device shows the same trends between the shape/scale factors and R_{ON} , that is, β_V , β_I , and $V_{\text{RESET}63\%}$ are roughly constant, while $I_{\text{RESET}63\%}$ is proportional to $1/R_{\text{ON}}$. The five devices show a good reproducibility of the observed trends.

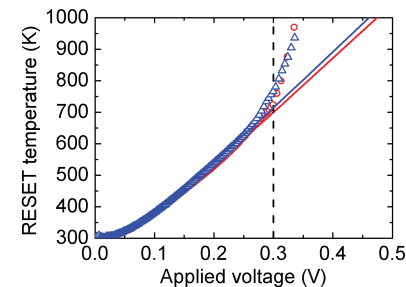


Fig. 4. Evolution of the experimental (circles and triangles) and theoretical RESET temperatures (continuous lines) of two RESET cycles in the HfO₂ device. The vertical dashed line indicates the same RESET applied voltage ($V_{\text{app},\text{RESET}} = 0.3 \text{ V}$) obtained from the maximum current criterion.

adequately controlling the SET process to reduce the variability of R_{ON} .

Fig. 3 shows that $V_{\text{RESET}63\%}$ remains independent of R_{ON} , while $I_{\text{RESET}63\%}$ scales with $1/R_{\text{ON}}$, as expected from the scatter plots of Fig. 1. On the other hand, the shape factors (β_V and β_I) appear to be independent of R_{ON} . Though the change of the scale factors of V_{RESET} and I_{RESET} distributions with R_{ON} is the same for both HfO₂ and NiO-based devices, the behavior of the shape factors is completely different because in the case of NiO, β_V and β_I were reported to scale with $1/R_{\text{ON}}$ [10]. In [10], a physics-based model was proposed for the RESET statistics. This model implements the idea that in order to fully RESET the CF, out-diffusion of all the N_{DEF} defects that form the CF narrowest constriction bottleneck is required.

Here N_{DEF} is defined as Nnn_{DEF} , with N being the number of slices that composing the CF bottleneck, n being the number of cells in each slice, and n_{DEF} the average number of defects in each cell. Departing from this idea, it was demonstrated that β_V and β_I should be proportional to $N_{\text{DEF}} \propto 1/R_{\text{ON}}$. This prediction was shown to be consistent with the results of NiO-based RRAM, but it is not consistent with the HfO₂ results reported in this letter. The reasons behind this discrepancy can be found by discussing the meaning of the RESET criteria and looking at the details of what happens before the RESET point. If there is no degradation of the CF before the RESET point, then the RESET event should be regarded as representing the initial step of the CF dissolution, that is, the out-diffusion of the first conductive defect from the CF bottleneck. In this case, a result like that reported for HfO₂ (i.e., β_V and β_I being independent of R_{ON}) would be consistent with the model of [10]. To explore the degradation occurring in the CF prior to the RESET point, we designed a methodology based on calculating the maximum CF temperature by means of two different procedures [11]. First, we consider a linear temperature dependence of the CF typical of metallic behavior, that is, $R_{\text{ON}}(T_{\text{MAX1}}) = R_0[1 + \gamma\alpha(T_{\text{MAX1}} - T_0)]$, where R_0 is the CF resistance at ambient temperature T_0 , γ is a geometrical parameter ($\gamma = 2/3$ for a cylindrical CF), and α is the experimental resistance-temperature coefficient. Using this equation, we can extract T_{MAX1} as a function of the applied voltage departing from the experimental evolution of R_{ON} , that is, using the CF as a self-thermometer. That is why we denote T_{MAX1} as the experimental temperature. On the other hand, we can also calculate the evolution of the maximum temperature as a function of the applied voltage from the heat dissipation equation, that is, $T_{\text{MAX2}} = T_0 + (R_{\text{TH}}/R_{\text{ON}})V^2$ where the $R_{\text{TH}}/R_{\text{ON}}$ ratio is assumed to be given by the Wiedemann–Franz law, that is, $R_{\text{TH}}/R_{\text{ON}} = (8\zeta LT_{\text{MAX2}})^{-1}$, with $L = 2.45 \times 10^{-8} \text{ W}\Omega/\text{K}^2$ being the Lorentz number and ζ a fitting parameter that allows us to trim the thermal resistance so as to ensure that $T_{\text{MAX1}} = T_{\text{MAX2}}$ at low voltages, where all the conductance change is due to temperature effects. Since no experimental data are involved in the calculation of T_{MAX2} , we have denoted it as the theoretical temperature. In the case of NiO, we concluded that significant degradation occurs before the RESET point, because these two temperatures diverge well before the maximum of the RESET current. In the present HfO₂-based devices, the results are quite different since, as shown in Fig. 4, the experimental and theoretical CF temperature curves nearly coincide before the RESET point ($V_{\text{app,RESET}} = 0.3 \text{ V}$, which corresponds to the maximum current). This means that, contrary to what was reported for NiO-based structures, in case of the present HfO₂-based devices, the RESET point nearly coincides with the starting point of the CF dissolution and the CF suffers little structural degradation before RESET, which explains the different behavior of β_V and β_I versus R_{ON} .

IV. CONCLUSION

The statistical distributions of RESET voltage and current in Pt/HfO₂/Pt RRAM devices were reported to be controlled by the distribution of initial CF resistance (i.e., by the ON-state resistance). Contrary to our previous

report for NiO-based structures, the Weibull slopes of the RESET voltage and current distributions were found to be independent of the CF resistance, thus indicating that the RESET point captures the initial stage of the CF dissolution process. The dependence of the scale factors on R_{ON} was found to be consistent with the thermal dissolution model of unipolar RESET. An intrinsic connection between the SET and RESET statistics was reported, because the spread of the RESET current statistics was directly determined by the distribution of ON-state resistance. Hence, it was concluded that the control of the ON-state resistance distribution is of great importance in order to achieve good uniformity of the RESET parameters and good performance of RRAM.

REFERENCES

- [1] R. Waser, R. Dittmann, G. Staikov, and K. Szot, “Redox-based resistive switching memories—nanionic mechanisms, prospects, and challenges,” *Adv. Mater.*, vol. 21, nos. 25–26, pp. 2632–2663, Jul. 2009.
- [2] H. Akinaga and H. Shima, “Resistive random access memory ReRAM based on metal oxides,” *Proc. IEEE*, vol. 98, no. 12, pp. 2237–2251, Dec. 2010.
- [3] G. W. Burr, B. N. Kurdi, J. C. Scott, C. H. Lam, K. Gopalakrishnan, and R. S. Shenoy, “Overview of candidate device technologies for storage-class memory,” *IBM J. Res. Develop.*, vol. 52, nos. 4–5, pp. 449–464, Jul.–Sep. 2008.
- [4] D. S. Jeong, R. Thomas, R. S. Katiyar, J. F. Scott, H. Kohlstedt, A. Petraru, and C. S. Hwang, “Emerging memories: Resistive switching mechanisms and current status,” *Rep. Progr. Phys.*, vol. 75, no. 7, p. 076502, Jun. 2012.
- [5] Y. Wang, Q. Liu, S. Long, W. Wang, Q. Wang, M. Zhang, S. Zhang, Y. Li, Q. Zuo, J. Yang, and M. Liu, “Investigation of resistive switching in Cu-doped HfO₂ thin film for multilevel non-volatile memory applications,” *Nanotechnology*, vol. 21, no. 4, p. 45202, Jan. 2010.
- [6] H. Y. Lee, Y. S. Chen, P. S. Chen, P. Y. Gu, Y. Y. Hsu, S. M. Wang, W. H. Liu, C. H. Tsai, S. S. Sheu, P. C. Chiang, W. P. Lin, C. H. Lin, W. S. Chen, F. T. Chen, C. H. Lien, and M. J. Tsai, “Evidence and solution of over-RESET problem for HfOX based resistive memory with sub-ns switching speed and high endurance,” in *Proc. IEEE Int. Electron Devices Meeting*, Dec. 2010, pp. 19.7.1–19.7.4.
- [7] J. Lee, J. Shin, D. Lee, W. Lee, S. Jung, M. Jo, J. Park, K. P. Biju, S. Kim, S. Park, and H. Hwang, “Diode-less nano-scale ZrO_x/HfO_x RRAM device with excellent switching uniformity and reliability for high-density cross-point memory applications,” in *Proc. IEEE Int. Electron Devices Meeting*, Dec. 2010, pp. 452–455.
- [8] C. Cagli, J. Buckley, V. Jousseaume, A. Salaun, H. Grampeix, J. F. Nodin, H. Feldis, A. Persico, P. Lorenzi, L. Massari, R. Rao, F. Irrera, T. Cabout, F. Aussemac, C. Carabasse, M. Coué, L. Perniola, P. Blaise, F. Zheng, Y. H. Yu, G. Ghibaudo, D. Deleruyelle, M. Bocquet, C. Müller, A. Padovani, O. Pirrotta, L. Vandelli, L. Larcher, G. Reimbold, and B. de Salvo, “Experimental and theoretical study of electrode effects in HfO₂ based RRAM,” in *Proc. IEEE Int. Electron Devices Meeting*, Dec. 2011, pp. 28.7.1–28.7.4.
- [9] X. Guan, S. Yu, and H. S. P. Wong, “On the switching parameter variation of metal-oxide RRAM-Part I: Physical modeling and simulation methodology,” *IEEE Trans. Electron Devices*, vol. 59, no. 4, pp. 1172–1182, Apr. 2012.
- [10] S. Long, C. Cagli, D. Ielmini, M. Liu, and J. Suñé, “Reset statistics of NiO-based resistive switching memories,” *IEEE Electron Device Lett.*, vol. 32, no. 11, pp. 1570–1572, Nov. 2011.
- [11] S. Long, C. Cagli, D. Ielmini, M. Liu, and J. Suñé, “Analysis and modeling of resistive switching statistics,” *J. Appl. Phys.*, vol. 111, no. 7, pp. 074508-1–074508-19, Apr. 2012.
- [12] U. Russo, D. Ielmini, C. Cagli, and A. L. Lacaita, “Self-accelerated thermal dissolution model for reset programming in unipolar resistive-switching memory RRAM devices,” *IEEE Trans. Electron Devices*, vol. 56, no. 2, pp. 193–200, Feb. 2009.
- [13] D. Ielmini, C. Cagli, and F. Nardi, “Physical models of size-dependent nanofilament formation and rupture in NiO resistive switching memories,” *Nanotechnology*, vol. 22, no. 25, p. 254022, Feb. 2011.